

COMPARATIVE ASSESSMENT OF THE FORCE PREDICTION ABILITIES OF SOME SINGLE EDGE ORTHOGONAL CUTTING MODELS OVER DIVERSE DATA

Patri K. Venuvinod and M.K. Cheng

Department of Manufacturing Engineering and Engineering
Management, City University of Hong Kong, 81 Tat Chee Avenue,
Kowloon, Hong Kong

ABSTRACT

The relative force prediction abilities of some well-known ANN-based, empirical and analytical models are assessed against several independent datasets by taking the *rms* error of cutting and thrust forces over all the datasets as the criterion. Progressing beyond mere data analysis, attention is paid to issues concerning how the model parameters themselves could be numerically modeled. A methodology for avoiding the need for measuring the shear angle, ϕ , is also developed. Model coefficients are estimated through nonlinear constrained optimization techniques. For estimating ϕ , the fractional variation of an idealized material invariant such as the mean shear stress, τ , on the shear plane is minimized subject to Hill's classical constraints. Several hitherto unknown insights regarding the relative effectiveness of each of the models have emerged. For example, it is found that the ϕ -values estimated from the measured forces alone are superior to those determined from chip measurements in the traditional manner.

NOTATION

a	the first constant in LinSAS, deg.
	chip load (cut area), m^2
A_s	area of shear plane, m^2
(ARFPE) _i	<u>A</u> ggregate <u>R</u> elative <u>F</u> orce <u>P</u> rediction <u>E</u> ffectiveness of model <i>I</i>
b	the second constant in LinSAS

e_{ij}	rms force prediction error of model i over dataset j , N
e_{ijk}	rms force prediction error of model i for record k of dataset j , N
ELinSAS	<u>Extended Linear Shear Angle Solution</u> : LinSAS but with a and b expressed as Powerfun
f_C, f_T	total cutting and thrust force respectively acting on the tool, N
f_{Ccf}, f_{Tcf}	clearance face cutting and thrust force respectively, N
f_{Cr}, f_{Tr}	rake face cutting and thrust force respectively, N
f_{Cjk}, f_{Tjk}	measured cutting and thrust force respectively in record k of dataset j , N
$f_{Cijk,pr}, f_{Tijk,pr}$	predictions by model i of f_C and f_T corresponding to f_{Cjk} and f_{Tjk} respectively, N
F_{cf}	clearance face friction force, N
F_{rf}	rake face friction force, N
F_s	shear plane shearing force, N
i	model index
j	dataset index
k	data record index within a given dataset
K_{cf}	magnitude of N_{cf} for unit v_i , N/m ³
K_{rf}	magnitude of N_{rf} for unit A_c , N/m ²
LFPT	<u>Linear Force Partitioning Technique</u>
LinSAS	<u>Linear Shear Angle Solution</u> of the form $\phi = a - b(\beta - \gamma)$
n_m	number of models available, i.e., the maximum value of I
n_d	number of datasets available, i.e., the maximum value of j
n_{rj}	number of records in dataset j
MVMI	<u>Minimizing the Variation of the Material Invariant</u> in the given model
N_{cf}	clearance face normal force, N
\bar{N}_{cf}	magnitude of N_{cf} per unit w_c , N/m
N_{rf}	rake face normal force, N
N_s	shear plane normal force, N
O	objective function
OFPT	<u>Optimized Force Partitioning Technique</u>
p	penetration of a dull cutting edge into the work surface, m
PowerFun	<u>Power Function</u>
r_e	tool cutting edge radius, m
rms	root mean square
(RFPE) _{ij}	<u>Relative Force Prediction Effectiveness</u> of model i over dataset j
s	uniform shear stress on lower boundary of shear zone, Pa
s_{Db}	value of s stored in model coefficient database, Pa
t_c	cut thickness, m
UoIFun	<u>University of Illinois Function</u>
v_i	clearance face interference volume, m ³
V	relative velocity between tool and workpiece, m/min
w_c	cut width, m
β	rake face (tool-chip interface) friction angle, deg.

γ	tool rake angle, deg
η	cutting effectiveness (= ratio of minimum and actual cutting energies under identical cutting conditions)
ϕ	shear angle, deg.
$\phi_{L Bj k}, \phi_{U Bj k}$	lower and upper limits respectively on ϕ for record k of dataset j
ϕ_m	shear angle determined from measured chip dimensions, deg.
μ_{cf}, μ_{rf}	coefficient of friction at clearance face and rake face respectively
θ	= $\beta - \gamma$, deg.
τ	mean shear stress on shear plane, Pa
τ_{Db}	value of τ stored in model coefficient database, Pa
ξ	a machining parameter (= $\tau A_c / f_c$)

INTRODUCTION

The current practice of relying on machining databases (e.g., [1]) for the purpose of anticipating process outputs such as cutting forces, temperatures, and tool life is highly unsatisfactory. A recurring theme at the CIRP-sponsored International Workshops on Modeling of Machining Operations being held since 1997 concerns the urgent need for reliable and robust predictive models of practical cutting operations so as to avoid the need for very large machining databases. As a result, industrial and academic communities have collaborated through a project coordinated by the National Institute for Standards and Technology (NIST) of the USA so as ‘to assess the ability of state-of-the-art machining models to make accurate predictions of the behavior of practical machining operations based upon the knowledge of machining parameters typically available on a modern industrial shop floor [2].’ There have also been suggestions to develop a ‘House of Models’ consisting of models that are declared by CIRP to be ‘fit to use’ in the metal cutting industry [3].

However, predictive modeling is not easy because machining processes continue to be poorly understood owing to the following reasons: the large variety of processes, input variables, internal variables, and output variables; the resulting large variety of chip types and forms; the high complexity of tool/work interface; the difficulty of determining work material properties at the extreme conditions prevailing in the cutting zone; the small scale of machining; and the fact that the process of chip formation is not uniquely defined [4].

The ability to anticipate the technological performance of manufacturing processes from different viewpoints is important in every process-planning phase (planning, monitoring, and control). Machining process performance measures of wide interest include cutting forces, power, temperatures, tool life, accuracy, and surface finish [5]. Of these, cutting forces are of particular importance since they influence the rest of performance measures strongly. For instance, while programming a computer controlled numerical (CNC) machine to produce a part of specified geometry and accuracy, knowledge of the likely magnitudes of the

quasi-static cutting force components along the machine axes is essential for ensuring that the torque/power capacities of the axis-drives are optimally utilized during roughing passes and that the cutter path is duly compensated during the finishing pass so as to achieve the desired part accuracy notwithstanding the geometric, thermal and force-induced deflection errors associated with the particular machining set up [6].

A wide variety of machining operations are in industrial use today. It is unrealistic to seek to develop an independent model for each of these ‘practical’ operations. It might be more reasonable to model each practical operation in terms of a common and simplified machining operation. Armarego (among a few others) has suggested that this should indeed be possible if one uses a model parameter database compiled on the basis of data collected from single edge orthogonal cutting experiments performed using the same work-tool material combination as used in the practical operation. Based on this premise, he systematically covered one practical machining after another—e.g., turning [7], end milling [8], and drilling [9].

Approaches to cutting force modeling of single edge orthogonal cutting differ substantially. Many models express the cutting force components associated with each work-tool combination as explicit analytical functions of the input conditions (e.g., cutting speed, V ; cut area, A_c , etc). A popular function is the power function where the function coefficients are determined through nonlinear regression performed against the measured cutting forces. The model coefficient database facilitates the prediction of the cutting forces likely to arise when a new set of cutting conditions is applied. Inevitably, since the exercise has to be repeated for each work-tool combination, this process requires a very large and expensive model coefficient database to be built.

A general drawback of the empirical approach is that it treats the machining process as a black box. No prior knowledge concerning the physics of the process is assumed to be available. This scenario has changed substantially since the seminal works of Merchant [10, 11] who introduced certain physical principles related to the plastic deformation of metals. He idealized chip formation as a process resulting from shear at a single shear plane. Assuming that the work material is perfectly plastic, he considered the shear stress, τ , on the shear plane to be a work-material invariant. (This assumption is now generally recognized to be an oversimplification that does not explicitly take into account the implications of the possible triaxial state of stress and high strain rates encountered in metal cutting. However, Armarego [7] and a few others have observed that the assumption of τ being constant for a given work material holds quite well provided that the total cutting force is properly partitioned into components arising from the specific phenomena occurring at the rake and clearance sides.)

Subsequently, more complex physics-based models were developed for single edge orthogonal cutting. These models are commonly known as ‘analytical’ models since they have been mainly used to analyze input-output relationships so as to gain a deeper understanding of the chip formation

mechanisms involved. Such an understanding is essential while conducting downstream exercises directed towards the estimation of cutting temperatures, tool wear, etc. The advantage of the ‘analytical’ approaches “is that predictions are made from [certain] basic physical properties of the tool and workpiece materials together with the kinematics and dynamics of the process. Thus, after the appropriate physical data [are] determined, the effect of changes in cutting conditions (e.g., tool geometry, cutting parameters, etc.) on industrially relevant decision criteria (e.g., wear rate, geometric conformance, surface quality, etc.) can be predicted without the need for new experiments. If robust predictive models can be developed, this approach would substantially reduce the cost of gathering empirical data and would provide a platform for a priori optimization of machining process parameters based upon the physics of the system [2].”

More recently, computational approaches based on finite element or finite difference techniques have been developed. However, a round robin exercise conducted by CIRP identified several unresolved problems with these approaches [4]. Hence, it is likely that, at least in the near time future, one would have to continue to rely on analytical models.

Whenever we attempt predictive modeling of a machining operation, we are putting faith in the high likelihood of the cutting process being inherently repeatable. However, often, the facts are otherwise. For instance, consider the single edge orthogonal cutting data reported by Ivester *et al.* in 2001 to support the CIRP International Competition on ‘Assessment of Machining Models’ [2]. The experiments were replicated at four different laboratories while utilizing tubular workpieces and tool inserts drawn from the same batches. Interestingly, although extraordinary care was taken while performing the experiments, there was significant variation (up to 50%!) in the ratio of the measured cutting force range across the four laboratories to the mean value.

Hill was amongst the first to recognize the inherent variability of machining processes [12, 13]. In particular, he wondered why the extant theories of machining did not generally agree with experiments. Was it because the assumptions underlying the models were unrealistic? Or, was it because experimental techniques were inadequate? Or, were the theories unsound, even within their self-imposed limits? Hill focused on the last aspect by envisaging that “the possibility of uniqueness [in machining] is fruitless: that is, there may be many, even infinitely many, steady state configurations of a given type (e.g., with a single plane of shear or with a ‘false cap’ of given shape adhering to the tool). Indeed, in a process such as machining where there is little constraint on the flow, it seems certain that the initial conditions must influence the ultimate steady state. Granted this, the logical approach to the problem is radically different. The ultimate objective now becomes not single unique solution, but a whole range of steady-state solutions of (let us say) the shear-plane type, each complete in the technical sense and each associated with a set (or sets) of initial conditions by an intervening nonsteady transitional flow [13].” Next, by excluding configurations that imply overstressing of materials at the singularities of stress within the deformation zone in machining, Hill arrived at permissible

ranges of shear angle, ϕ , in single edge orthogonal cutting as functions of rake angle, γ , and the apparent coefficient of friction, μ_{rf} , at the rake face.

If we accept Hill's views, the prospects of predictive modeling seem hopeless. Yet, the record shows that some models have been able to make fairly good force predictions in the context of certain datasets. For instance, a closer examination of the datasets reported in [2] indicates that the data from each individual laboratory are internally consistent to a fair degree. Yet, there are substantial differences between the force values measured by different laboratories. This may be explained by the fact that the initial conditions are strongly dependent on the machining setup used but, for a given setup, are reasonably repeatable over a limited period. Indeed, there is some hope for predictive modeling of cutting forces!

Among the analytical cutting force models directed towards single edge orthogonal cutting operations resulting in continuous chips without the formation of a built-up-edge (type II chips), the models developed by Armarego [7], DeVor and Kapoor [14, 15], Kobayashi and Thomsen [16-19], Oxley [20-23], and Rubenstein [24, 25] are particularly noteworthy.

However, generally, these modelers had used their own specifically collected data to validate their specific models. This raises two concerns. Firstly, there is always the possibility of experimental bias in favor of the model being validated. Secondly, it is not unreasonable for the modeler-experimenter to select experimental conditions that are likely to result in a cutting process that ensures as much agreement as possible between the process-related assumptions that the modeler had made and the actual process. For instance, input conditions might have been selected to ensure type II chips. This is acceptable if the objective is just to validate the model, but not for the purpose of predictive modeling. One would like the model to be reasonably robust, i.e., work in an adequate manner under shop floor conditions where it is quite possible to encounter a wide variety of chip-states (including and beyond type II).

It follows from the above discussion that, from a predictive modeling perspective, it is highly desirable to make a comparative assessment of all credible cutting models against a common (and large) collection of independently compiled datasets. However, to date, no such exercise has been undertaken. An objective of this paper is to fill this gap. In the present work, twelve distinct datasets drawn from literature are utilized for the purpose of assessing two artificial neural network-based approaches, two empirical modeling approaches, and fourteen analytical approaches inspired by the works of Armarego, DeVor and Kapoor, Kobayashi and Thomsen, and Rubenstein.

This paper proceeds beyond mere model assessment by pursuing two further objectives. The first is motivated by the observation that almost all currently available analytical cutting models assume that each data record includes, in addition to the cutting force magnitudes, the value of the shear angle, ϕ .

Cutting force measurement is usually not a problem. For instance, as noted by the present authors in [26], cutting force monitoring is easily automated

by sensing machine axis motor currents with the help of Hall-effect sensors. In contrast, traditional methods of estimating ϕ involve some manual dimensional measurement of chips. This is a process that is tedious, expensive, prone to significant error, and difficult to automate. Clearly, the need for measuring ϕ is the greatest single obstacle to the assimilation of cutting force models in industry. However, very few modelers (with the rare exception of [19]) have addressed this issue. This paper proposes a new method of estimating ϕ solely from measured forces corresponding to known input conditions. The method utilizes a new principle called MVMI (Minimize the Variation of the Material Invariant) subject to Hill's classical constraints on ϕ [13] for a given work material.

The second objective is motivated by the observation that many of the currently available models have been configured mainly to enable analyses of individual data records (input-output combinations) to arrive at sets of model parameters that are plausible when exactly those input states are present. Next, the patterns implicit in the model parameters are approximated by explicit analytical functions (e.g., the power function). These functions are then utilized for the purpose of cutting force prediction for a new input condition. However, it can be anticipated that different functional relationships will result in different degrees of distortion. Hence, this paper includes a comparative assessment of some functions suitable for storing model parameter patterns. The next five sections discuss some issues of common interest to all predictive modeling approaches examined in the present work.

LINEAR AND OPTIMIZED CUTTING FORCE PARTITIONING

Early modelers of machining operations had assumed that the cutting tool was perfectly sharp (e.g., [10,11]). Hence the measured cutting forces, f_C and f_T , could be attributed entirely to chip formation. Subsequent researchers (e.g., [7, 24]) argued that practical cutting tools are always dull, i.e., their cutting edges would be rounded and possibly exhibit a flank wear land. Owing to the roundness of the edge, the local rake angles in the vicinity of the work surface would be highly negative so that it becomes easier for some of the work material approaching the rounded edge to be extruded towards the workpiece instead of moving over the rake face as a part of the chip. This process would give rise to parasitic forces (i.e., to forces that do not directly arise from chip formation) on the clearance face side of the tool (Figure 1). In short, it is necessary to partition the total forces into those on the rake side, f_{Crf} and f_{Trf} , and those on the clearance face side, f_{Ccf} and f_{Tcf} . Hence, only the rake side forces should be used while performing an equilibrium analysis of the chip. Otherwise, there would be significant errors.

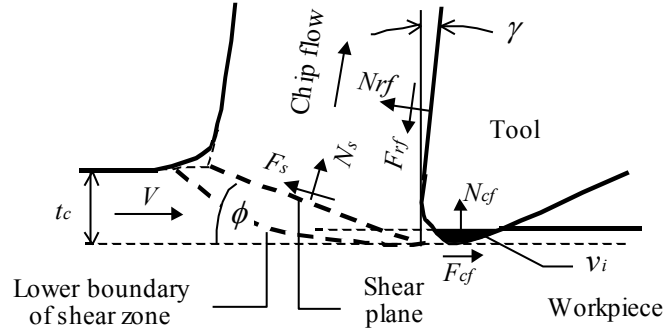


Figure 1. Single edge orthogonal cutting.

There exist several alternative approaches to solving the force-partitioning problem. Armarego and Rubenstein (among others) presented empirical evidence suggesting that, as an approximation, both f_C and f_T can be taken to be increasing in a linear fashion with cut thickness, t_c when other conditions remain the same [7, 24]. The linear regression lines for f_C and f_T usually have positive intercepts along the respective force axes and these intercepts may be taken to be equal to f_{Ccf} and f_{Tcf} respectively. The rake side force components can then be estimated as $f_{Crf} = f_C - f_{Ccf}$ and $f_{Trf} = f_T - f_{Tcf}$. In the rest of this paper, we will refer to this force partitioning procedure as LFPT (the Linear Force Partitioning Technique).

A radically different approach to force partitioning has been developed more recently by Endres, DeVor and Kapoor [14, 15]. The parasitic forces on the clearance side arise mainly because of the penetration of the rounded cutting edge into the work material (see Figure 1). This results in certain ‘interference volume,’ v_i , between the tool and the workpiece, the magnitude of which is easily calculated once we assume a certain ‘penetration depth’, p , of the dull edge into the work surface. Endres *et al.* then develop an expression for v_i in terms of p , r_e , and the tool clearance angle. Next they express K_{rf} , μ_{rf} , μ_{cf} , K_{cf} , and p in terms of input conditions (γ , t_c , and V) using the following functional form (explanations of these symbols are provided in the Notation section):

$$\text{model variable} = e^{(x_1 + x_2 \gamma)} t_c x_3 V x_4 \quad (1)$$

subject to a plausible set of constraints on the coefficients, x_1 to x_4 , corresponding to each of the modeled variables. In the rest of the present paper, we will refer to the functional form contained in equation 1 as ‘UoIFun’, i.e., the University of Illinois Function, signifying the affiliation of its principal proponents. Next, the magnitudes of the twenty model coefficients are determined by following a ‘multi-level, multi-pass iterative calibration algorithm’ that seeks to minimize the total error of machining force predictions. The procedure is more easily applied when the input dataset is relatively small in size [27].

After applying their force partitioning procedure to a selection of sixteen data records from the dataset reported in [28] for SAE 1112 ‘as received’ steel, Endres *et al.* arrived at several conclusions that did not agree with those of

Armarego and Rubenstein. In particular, they observed that, for the same tool (i.e., a tool with apparently the same cutting edge radius), ‘increasing the chip thickness strongly increases the thermal energy generated and hence transferred to the workpiece surface. This is reflected by increased tool penetration dominating over the decreased resistance to such penetration, which causes the clearance face forces to increase substantially with chip thickness [15].’ An implication of this observation is that the assumption of the linear force- t_c relationship that underpins LFTP cannot be generally valid.

Although it was not highlighted in their publications, a major drawback of the force partitioning approach of Endres *et al.* is that it requires prior knowledge of the cutting edge radius, r_e . The determination of this tool characteristic is extremely tedious, error prone, and difficult to automate. For the approach to succeed in an industrial setting, it is essential to overcome this difficulty. With this objective, the present authors have modified the approach of Endres *et al.* in the following manner:

- Model K_{rf} , μ_{rf} , μ_{cf} , and \bar{N}_{cf} . (Instead of modeling K_{cf} as in [14,15], we model \bar{N}_{cf} so as to avoid the need for knowing r_e .)
- We now have only sixteen parameter function coefficients to determine instead of the original twenty. In principle, these sixteen coefficients may be estimated using a numerical procedure analogous to the multi-level, multi-pass iterative process detailed in [27]. However, it appears possible to solve the problem more elegantly by applying certain well-known techniques of constrained nonlinear optimization. In particular, we have found it convenient to use the Interior Point and Exterior Point Penalty Function Methods described in [29]. Several mathematical software packages (e.g., MATLAB) have a library of standard routines to execute such optimization. The objective function to be minimized is still the total force prediction error over all the data records in the given dataset. Likewise, the constraints used by Endres *et al.* on the model parameter function coefficients are retained.

In the rest of the present paper, we will refer to the above modification of the method of Endres *et al.* as the OFPT (Optimized Force Partitioning Technique).

Before leaving the subject of force partitioning, it is necessary to stress that not all cutting modelers find it necessary to partition forces. For instance, Kobayashi and Thomsen [16-18] suggest that the magnitude of the shear stress on the shear plane, τ , may be taken as the slope of the linear regression line between the shear plane shearing force, F_s , and shear plane area, A_s . They also make the empirical observation that this regression line usually has a positive intercept, F_{s0} , on the F_s -axis. However, although Kobayashi and Thomsen were aware that this intercept could be explained via the ‘ploughing’ effect arising from a dull cutting edge, they attributed it to ‘size effect’ and/or the possibility that the “shear plane area [being] actually larger than that determined from chip measurements because of the fact that some bulging occurs at the free surface of the chip where the shear plane terminates. This bulging is described as flow ahead of the shear plane [16].”

NUMERICAL MODELING OF CUTTING FORCE MODEL PARAMETERS

An attractive feature of the cutting force model developed by Endres *et al.* [14, 15] is that, right at the beginning, the parameters such as K_{rf} , μ_{rf} , μ_{cf} , and K_{cf} that are essential during the subsequent force prediction phase are expressed as UoIFuns and the corresponding coefficients for each work-tool material combination stored in a database to facilitate subsequent force prediction

In contrast, the published works of most other modelers (e.g., Kobayashi, Armarego and Rubenstein) do not explicitly clarify how their respective cutting force model parameters may be expressed as functions of input conditions. They simply present their data analysis methods that yield arrays of individual values (instances) of the model parameters. By themselves, such arrays do not enable prediction except when the input conditions are identical. When the new input conditions are different, one has to interpolate/extrapolate by recognizing the patterns embedded within the parameter values. This requires the parameter arrays to be modeled using a suitable analytical function. One way is to use UoIFun (see equation 1). Another is to use a power function such as the following (called PowerFun):

$$\text{modelvariable} = x_1 t_c^{x_2} V^{x_3} (\pi/2 - \gamma)^{x_4} \quad (2)$$

Note that the inclusion of the ‘ $\pi/2$ ’ term in equation 2 ensures discrimination between the effects of positive and negative magnitudes of γ .

Would these parameter-modeling strategies be equally effective in terms of force prediction accuracy? This is a question that has not received sufficient attention so far. This issue will be discussed later.

EXTENDED SHEAR ANGLE SOLUTION

While implementing modeling approaches such as those due to Armarego, Rubenstein, and Kobayashi for the purpose of force prediction, it is necessary to model not only parameters such as μ_{rf} , μ_{cf} , and \bar{N}_{cf} but also the measured shear angle, ϕ_m . Whatever model we use, we would like the model estimates of ϕ_m to be close to the corresponding raw ϕ_m values. However, this does not appear to be a straightforward task.

Consider Figure 2 showing the results of expressing ϕ_m as a PowerFun. The data are taken from the 188 data records compiled from single edge orthogonal cutting experiments performed using 18-4-1 HSS tools on SAE 1112 ‘as received’ work material [28]. Clearly, the result is unsatisfactory. While we would like to see a linear regression line with its slope close to unity and

intercept close to zero, the actual regression line is highly nonlinear. We obtained similar negative results when we adopted UoIFun.

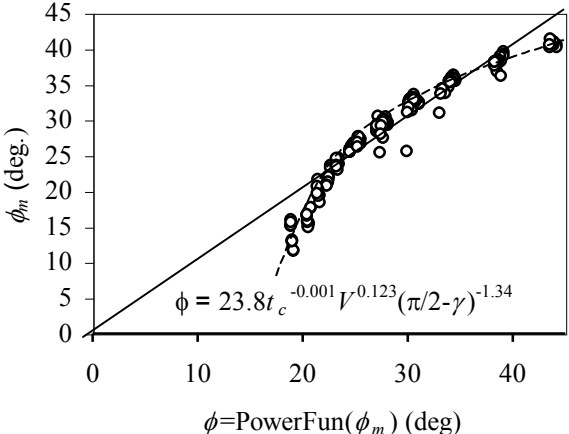


Figure 2. Effectiveness of modeling ϕ as PowerFun
(Data from [28], SAE1112 as received, 18-4-1 HSS, Approach Ar1 from Table 4).

In classical orthogonal machining literature, linear shear angle solutions (LinSAS) of the following general form have often been used with some degree of credibility:

$$\phi = a - b(\beta - \gamma), a \leq 45^\circ, b \geq 0.5 \tag{3}$$

where a and b are appropriate constants, β is the tool-chip friction angle and γ is the rake angle.

For instance, Merchant [11] developed his first shear angle solution by invoking the principle of minimum energy in conjunction with his idealization of orthogonal cutting as a shearing process occurring over a shear plane in the presence of a perfectly sharp cutting edge. This approach resulted in the LINSAS with $a=45^\circ$ and $b=0.5$. However, this solution was not found to be in general agreement with empirical data—not necessarily because the principle of minimum energy is inapplicable but because the principle is applied in conjunction with an erroneous or oversimplified cutting model (e.g., the assumption that shear occurs over a single shear plane).

To appreciate the effectiveness of equation 3, consider Figure 3 where, for the same data as used in Figure 2, ϕ_m is plotted against $(\beta-\gamma)$ obtained via LFPT. Clearly, drawing a single straight regression line to determine the most appropriate values of a and b will lead to highly unsatisfactory results.

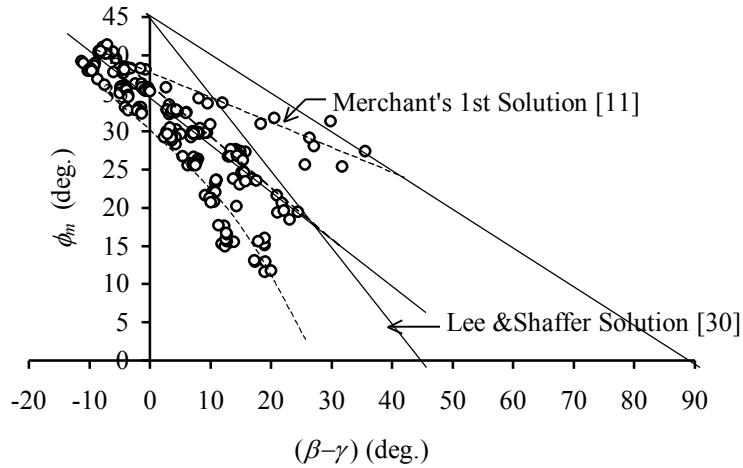


Figure 3. $(\beta-\gamma)$ from LFPT versus ϕ_m plot (Data: same as in Figure 2).

However, a closer examination of the data-points in Figure 3 reveals that they could be partitioned into three subsets each exhibiting a separate but approximately linear regression. This insight suggests that the linear shear angle solution could be ‘extended’ by expressing constants a and b as independent functions such as PowerFun. However, since t_c usually has negligible influence on the shear angle, we may ignore the t_c -terms in the two PowerFuns. Based on these observations, we now propose the following generalized form of the extended linear shear angle solution (ELinSAS):

$$\text{ELinSAS: } \phi = x_1 V^{x_2} (\pi/2 - \gamma)^{x_3} - x_4 V^{x_5} (\pi/2 - \gamma)^{x_6} (\beta - \gamma) \quad (4)$$

Figure 4 shows the effectiveness of applying ELinSAS to the data in Figure 2. Comparing it to Figure 2, it is clear that ELinSAS has yielded a substantially improved result.

SIDESTEPPING THE SHEAR ANGLE PROBLEM THROUGH ‘MVMI’

A major difficulty with most analytical models of cutting is that their application requires the magnitude of the shear angle, ϕ , corresponding to each data record to be known in advance. Usually, this is achieved through measurements of chip thickness, length, or weight. In any case, certain dimensional measurements performed on flattened chips cannot be avoided. However, dimensional measurement of a chip is a tedious process that is not easily automated. The significant manual effort required and the fact that the chip surface is usually quite rough makes the process highly error prone.

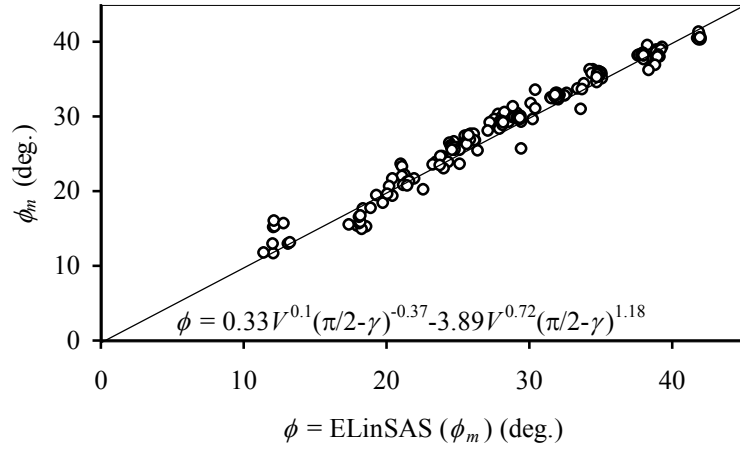


Figure 4. Effectiveness of the extended linear shear angle solution
(Data: same as for Figure 2).

The shear angle problem may be solved by utilizing some plausible physical principles to develop a ‘shear angle solution’ expressing ϕ as a function of some process parameters that can be directly computed from measured forces. For example, provided that we know the magnitudes of constants a and b, we can estimate the shear angle from the friction angle by using the linear shear angle solution described in equation 3. Over the last five decades, some fifty odd shear angle solutions have been developed. However, two problems remain. Firstly, the range of application of each shear angle solution seems to be limited. A given solution may work on some datasets but not others. Secondly, the solution coefficients still need to be calibrated against measured shear angles (as in the case of LinSAS as well as ELinSAS referred to in the previous section). Clearly, it is essential that we find a way of sidestepping the problem of shear angle measurement entirely.

Cumming *et al.* seem to be among the very few who have come close to sidestepping the problem. In [19], they argued that, quite frequently, f_T is found to be linearly related to f_C so that ϕ can be estimated by minimizing the overall deviation between the actual values and the values expected from the linear relationship. Thus, it was concluded that ‘no reference need be made to the actual angle ϕ , and better equivalent angles are determinable if a stiff but sensitive dynamometer is available.’ Cumming *et al.* also outlined a more generalized quadratic f_T versus f_C relationship but did not demonstrate its implementation.

The key idea behind Cumming’s approach consists of two steps. Firstly, based on plausible physical considerations, we identify a relationship among one or more key process variables that is likely to generally hold, i.e., remain invariant. Next, we determine the distribution of ϕ that minimizes the deviations (variance) from this relationship over all the data records under consideration.

An analytical modeler usually strives to arrive at generalizations that are expected to hold over a wide range of input conditions. Some generalizations are expected to hold for a particular work-tool material combination. Others are expected to hold irrespective of the tool material and cutting conditions as long as the work material remains the same. It appears that the most general (hence, the most ‘invariant’) among these is the work material related invariant. On this basis, we suggest that it should be possible to arrive at a likely distribution of shear angle simply by minimizing the fractional variation (the ratio of the standard deviation to the mean value) of the most significant work material ‘invariant’ involved in the model. Henceforth, we shall refer to this procedure as MVMI—Minimizing the Variation of the Material Invariant in the given model.

For instance, in the context of Armarego’s approach, MVMI takes the following form. First, we apply LFTP to determine f_{Crf} , f_{Trf} , f_{Ccf} , and f_{Tcf} values for each record k of dataset j . Next, we determine μ_{rf} , μ_{cf} , and \bar{N}_{cf} for all data records in the dataset. These values are then modeled using separate UoIFuns or PowerFuns through numerical nonlinear regression. Thus, $3 \times 4 = 12$ model parameter coefficients would have been determined at this stage. Next, we determine $\beta = \arctan(\mu_{rf})$ for all data records in the dataset. It is assumed that the ϕ -distribution across the dataset follows a single ELinSAS so that there will be six additional coefficients to be estimated. Next, we compute the lower and upper limits, ϕ_{LBjk} and ϕ_{UBjk} respectively of ϕ for each record k in dataset j using the equations developed by Hill in [13]. (The constraints placed on possible values of ϕ merely ensure that the optimization procedure does not converge to an unrealistic value of ϕ , e.g., $\phi \rightarrow 0$. Once, the extreme value has been avoided, the limits chosen have little influence on the value of ϕ to which the process of MVMI converges. It has been found that one can arrive at the same optimized values by using a different but plausible set of constraints on ϕ .)

Finally, we perform the nonlinear least squares optimization using the Exterior Point Penalty Method [29] that minimizes the following objective function, O :

$$O = \sum_{k=1}^{k=n_j} \tau_{jk} - \bar{\tau}_j + K_\phi \{ \delta_{LB} (\phi_{jk} - \phi_{LBjk})^2 + \delta_{UB} (\phi_{jk} - \phi_{UBjk})^2 \} \quad (5a)$$

where τ_{jk} is the estimate of τ for record k in dataset j , K_ϕ is a penalty constant

$$\bar{\tau}_j = \text{mean } \tau = \frac{\sum_{k=1}^{k=n_j} \tau_{jk}}{n_j}, \quad (5b)$$

ϕ_{LBjk} and ϕ_{UBjk} are the lower and upper limits respectively on ϕ for record k in dataset j , δ_{LB} is equal to 0 if $\phi_{jk} \geq \phi_{LB}$, else it is equal to 1, and δ_{UB} is equal to 0 if $\phi_{jk} \leq \phi_{UB}$, else it is equal to 1.

In contrast, Kobayashi and Thomsen's shear plane-based models of orthogonal cutting do not require force partitioning as a prerequisite for determining τ [16-19]. For a given dataset with constant work-tool material combination, τ is determined as the slope of the regression line between the shear force on the shear plane, F_s , and the area of shear plane, A_s . This τ is the work material invariant in this model. Hence MVMI for this model may be implemented by following essentially the same procedure as that described above for Armarego's model except that, while implementing MVMI, the scatter of the data points with respect to the F_s versus A_s regression line is minimized.

Notwithstanding the popularity of the shear plane approach, it must be emphasized that the notion of shear plane is only an approximation. Once we recognize a shear zone of finite thickness, shear strain rate and temperature would vary gradually across the shear zone. As a result, τ could also vary across the shear zone. In other words, a single value of τ might not suffice to characterize the influence of the work material on the cutting force magnitudes. Among the foremost practitioners of this approach are Oxley and his associates [20-23] who have moved away from the simplistic and semi-empirical view of constant τ by considering a host of variables associated with the shear zone of finite thickness and the tool-chip interface.

From the viewpoint of force prediction under shop floor conditions, shear zone-based approaches such as that of Oxley are difficult to implement. They require prior knowledge of several work material related parameters that are difficult to evaluate. This has to be done for each and every work material encountered on the shop floor. Besides, we have found it difficult to implement some of our optimization strategies (to be discussed later) in association with such shear zone based analyses. For these reasons, in the present paper, we have not attempted to assess the models developed by Oxley and his associates. We leave this issue to future researchers.

However, there is empirical evidence suggesting that, in many cutting situations, shear zone thickness decreases with increasing cutting speed (modern machining practice is tending towards higher and higher cutting speeds), so the shear zone can be assumed to be 'thin' and, hence, τ may be taken to be the model invariant.

In Rubenstein's approach [24, 25], the shear flow stress, s , along the lower boundary of the shear zone is the work material invariant. Rubenstein recognizes that there must always be a shear zone of finite thickness and assumes that the 'lower' boundary (the boundary away from the chip-side) of the zone is a slip line. He then presents arguments leading to the conclusion that, irrespective of the normal distribution on the lower boundary and whatever be the friction conditions at the tool-chip interface, s can be simply calculated in single edge orthogonal cutting as

$$s = f_{Cr} / \{A_c (\cot\phi + 1)\} \quad (6)$$

Note that the above equation includes ϕ merely for the purpose of enabling the results to be presented in a simple manner. Note also that, in contrast to the shear plane located somewhere in the *middle* of the shear zone, the lower

boundary is at the initial end of the shear zone. Hence, unlike τ , s should remain unaffected by the strain distributions within the shear zone although some temperature influence could still be present. Hence, s is the material invariant in this model. The major advantage of Rubenstein's approach is that, in contrast to τ , s can be determined without any reference to the friction coefficient, μ_{rf} , at the tool-chip interface and solely from f_{Cr} and ϕ . The disadvantage is that only f_{Cr} can be predicted and we need to invoke some other method to predict f_{Tr} .

AGGREGATE RELATIVE FORCE PREDICTION EFFECTIVENESS OF A MODEL

We may take the *root mean square* (rms) of the deviations between the predicted and measured forces as a measure of the prediction error of the model over the dataset. Thus,

$$\begin{aligned}
 & \text{IF model } i \text{ has succeeded in predicting} \\
 & \text{cutting forces with acceptable error over dataset } j, \\
 & e_{ij} = \text{rms force prediction error of model } i \\
 & \text{over all the records, } k = 1 : n_{rj} \text{ of dataset } j \\
 & = \sqrt{\frac{\sum_{k=1}^{n_{rj}} (f_{Cijk} - f_{Cjk})^2 + \sum_{k=1}^{n_{rj}} (f_{Tijk} - f_{Tjk})^2}{2(n_{rj} - 1)}} \quad (7)
 \end{aligned}$$

ELSE
 $e_{ij} = \text{NAN (Not a Number)}$
 (See Notation section for explanations of the symbols.)

Note that the above error estimate arises due to two reasons: data errors, and modeling errors. Data errors can be classified as those due to assignable causes (e.g., the dynamometer has not been properly calibrated, or an inadequate chip measurement technique has been applied) and random errors due to unknown causes. Likewise, modeling errors can be of different types. Firstly, not all the model assumptions might not be valid in the particular machining context. For instance, whereas the model has assumed type II chips, the actual chips might not be fully continuous. Or, there could be a built-up-edge present. Or, while the model assumes a thin shear zone to be present, the actual shear zone might be quite thick. Secondly, even though the model assumptions have been fully satisfied (a rare occurrence), the physical principles on which the model is based might be flawed to some degree. The model parameter estimates obtained from the data analysis phase would be that much in error. Thirdly, even if the model parameters have been estimated reasonably accurately, there could be varying degrees of error caused while we numerically model the parameters. We must remember that there is no specific physical basis underlying UoIFun, PowerFun, or ELinSAS. These functions might not always be capable of capturing fully the regularities implicit in the corresponding model parameter distributions. It is also possible that different kinds of regularities exist across different subsets of the same dataset. For instance, model parameter behavior at higher speeds could be very different from that in a lower speed range. Yet, we are trying to model both parts of the dataset using the very same functional form.

Finally, there is the possibility of the initial conditions being different across the dataset (recall Hill's arguments [13]) and the modeling procedure is unable to take into account the influence of variations in initial conditions.

We could assess a model in an absolute sense only when we have a dataset that is totally free of experimental errors. Our problem is that we can never hope to have such a 'perfect' dataset. Alternatively, if we have a 'perfect' model in hand, the e_{ij} estimate resulting from this 'perfect' model would entirely be data error. We would then know the variance due to data error. When we are assessing a different and less than perfect model, we can subtract the variance due to data error from the total variance so as to arrive at the corresponding variance due to modeling error. Again, our problem is that we could never hope to have a 'perfect' model available.

Clearly, the only recourse we have is to adopt a 'relativistic' approach. When we compare the performances of a set of imperfect predictive models over a specific imperfect dataset, the data errors are common across all model implementations. One of these model implementations would be the 'closest' to the unknown 'perfect' model. We may use (quite arbitrarily) this 'closest' model as the reference against which rest of the models are evaluated. The advantage of this approach is that, although we are unable to quantify the degree of perfection of a given model in an absolute sense, we will still be able to rank the available models in the order of their closeness to perfection.

Based on the above rationale, the following procedure is proposed for assessing the aggregate relative force prediction effectiveness (RFPE) of a given modeling approach:

$$\begin{aligned}
 & \text{IF } e_{ij} = \text{a real number} \\
 & \quad (RFPE)_{ij} = \text{relative force prediction effectiveness} \\
 & \quad \quad \quad \text{of model } i \text{ over dataset } j \\
 & \quad \quad \quad = \frac{\min(e_{ij})_{i=1}^{n_m} \text{ for dataset } j}{e_{ij}} \qquad (8)
 \end{aligned}$$

$$\begin{aligned}
 & \quad \quad \quad \text{[Note : Thus, } (RFPE)_{ij} \leq 1] \\
 & \text{ELSE} \\
 & \quad (RFPE)_{ij} = 0
 \end{aligned}$$

Note that the RFPE-values are meaningful only in the context of the specific sets of models and datasets over which the assessment exercise has been conducted. This must be borne in mind while drawing generalized conclusions from such an assessment exercise.

The above feature also highlights the futility of trying to build a "House of Models [3]" that exists on its own. As in much of nature, in the context of machining models too, 'fitness for purpose' is not universal. Since the work-tool material combinations normally encountered by different machines operating in different shop floors are likely to be quite diverse, one cannot expect the same predictive model to emerge as the 'winner' in every machining situation. Likewise, the initial conditions and ranges of cutting conditions could be quite different. Therefore, it is better to equip each shop floor machine with force prediction software that compares the performance of several competing models

from data that are continuously gathered by the specific machine. Each machine should be allowed to ‘discover’, in a Darwinian fashion, the model that has the ‘best fit’ with the environment in which it normally operates. However, if we insist on building a “House of Models” so as to promote the development of improved models, we would have to build a companion ‘House of Data’ too so as to act as a reference. One cannot exist without the other.

DATASETS

Table 1 details the twelve datasets used in the present comparative assessment (i.e., $n_d = 12$). Note that the order of datasets in the table has no significance. With 188 records, dataset 1 is the largest in Table 1. Eggleston *et al.* had collected these data in 1959 for the purpose of testing several shear angle solutions available at that time [28]. They appear to have been quite meticulous in measuring chip dimensions for the purpose of estimating ϕ . Their data indicated that LinSAS is only approximately satisfied and not all ϕ values fell within Hill’s limits. However, these observations were based on an analysis that had not invoked partitioning of the total forces between the rake and clearance sides. The way force partitioning is effected could result in different β values and, hence, in a different degree of agreement.

Datasets 6, 7, and 8 were collected by Ivester *et al.* in 2002 to support the CIRP International Competition on ‘Assessment of Machining Models [2]’. The experiments were replicated at four different laboratories with each laboratory using a different machine but utilizing workpieces and tool inserts drawn from the same batches. However, the input conditions spanned by each laboratory were not identical. Further, although great care was taken while performing the experiments, there were substantial differences in the f_C and f_T values recorded for nominally identical input conditions at different laboratories. For instance, for one particular input state, f_C was measured to be 580N by one laboratory and 980N by another laboratory! For this reason, while compiling the data records in datasets 7 and 8, we have used the average values of measured forces across the four laboratories. Further, the measurements of cutting forces and of shear angles were not conducted simultaneously, but with different input conditions at different times. Consequently, it could not be ensured that the initial conditions prevailing during the two exercises were the same. In view of these problems, we have ignored the shear angle values provided in [2]. As a result, we have been unable to assess modeling approaches Ar1, Ar2, R1, R2, KT1 and KT3 over datasets 6, 7 and 8 (see Tables 3 to 6).

Table 1. Dataset details.

j	Reference.	Work Material	Tool Material	γ deg	V m/min	t_c mm	w_c mm	n_{rj}
-----	------------	---------------	---------------	-----------------	--------------	-------------	-------------	----------

1	Eggleston <i>et al.</i> [28]	SAE 1112 as received	18-4-1 HSS	5 to 40	10 to 52	0.05 to 0.25	5.1	188
2		SAE 1112 annealed						78
3		2024 T4 Al		175 to 240	93			
4		6061 T6 Al		175	18			
5		Brass cd		20 to 40	144	0.05- 0.28	4.6	49
6	Ivester <i>et al.</i> [2]	AISI 1045 steel	K68 carbide, uncoated	-7 to +5	200 to 300	0.15 to 0.30	6	9 (Lab 1)
7			K68 carbide, Coated					52 (Labs 1-4)
8								56 (Labs 1-4)
9	Lapsley <i>et al.</i> [31]	Steel ar	HSS	25 to 45	27.4	0.06 to 0.22	12.1	20
10	Kececioglu [32]	SAE1015 118 BHN	steel cutting carbide	-10 to 36.5	38 to 227	0.1 to 0.3	4.3	22
11	Merchant [12]	NE9445 steel	carbide	-10 to 10	60 to 361	0.02 to 0.2	6.35	15
12	Crawford & Merchant [33]	SAE1020 hot rolled	18-4-1 HSS	0 to 50	19 to 159	0.16		24

Dataset 9 was collected by Lapsley, Grassi and Thomsen in 1950 [31] for the purpose of correlating plastic deformation of the work material in cutting with that under pure tension. Dataset 10 was collected by Kececioglu in 1958 for testing some prevailing models [32]. Datasets 11 and 12 were collected by Merchant in 1945 and 1953 respectively. The former was used by Merchant to demonstrate his chip-equilibrium model and his first shear angle solution. The dynamometer used in either case was of a primitive type using dial gages. Hence, one should be cautious in drawing generalizations from these two datasets.

Note that, in contrast to datasets 1 to 3, datasets 4 to 12 are quite small in size. We would like to model the influence of at least three variables (V , t_c , and γ) on cutting force magnitudes. One may also assume that the effects of each of these variables would be nonlinear in nature. Further, the process of determining model parameter coefficients in our procedure involves statistical nonlinear regression. Likewise, when we estimate shear angles via our MVM procedure, we need to employ a nonlinear constrained optimization procedure. Both these procedures work more robustly and converge with greater ease when n_{rj} is large.

It follows from the above discussion that it is more desirable to work with larger datasets rather than smaller ones. But, large datasets are expensive to compile in a laboratory setting that depends on manual chip measurements to estimate ϕ . Here lies the importance of the MVMI approach.

The realization that large datasets could facilitate predictive modeling of cutting operations is not immediately evident from cutting literature. For instance, as recently as in 1995, Endres *et al.* [14, 15] validated their modeling approach against a selection of just 16 data records drawn from the 188 data records available in Eggleston's 1959 data (dataset 1 in Table 1). The reason cited was computational efficiency.

FORCE PREDICTION USING ARTIFICIAL NEURAL NETWORKS

An analytical cutting model captures the patterns implicit in a given dataset by attempting to relate them to certain widely accepted principles of science. This approach is distinct from pattern recognition using an artificial neural network (ANN). An ANN is not equipped with any scientific knowledge. It is merely an algorithmic procedure that (hopefully) is capable of recognizing patterns implicit in a given set of data irrespective of their origin—based on process-physics, or otherwise. On the other hand, the advantage of using ANN-based modeling is that no assumptions need be made regarding the physics of the process. Hence, provided that a reasonably effective ANN algorithm has been used, we can expect the e_{ij} estimate from an ANN to be significantly smaller than that arrived at by an analytical model that, somehow, has to make the 'right' physical assumptions and use the 'right' scientific principles. In short, ANN-based modeling should be of help in arriving at the smallest possible estimate of e_{ij} .

In view of the above considerations, two ANN strategies have been implemented in the present work. Approach BPN uses a back propagation network (BPN)—see MATLAB 6.1 neural Network Tool Box for details—using three input nodes (V , A_c , and γ), four hidden nodes, and two output nodes (f_c and f_T).

The second is an adaptive neuro-fuzzy inference system (ANFIS). ANFIS is a four-layer neural network that simulates the working principle of a fuzzy inference system [34-36]. Our ANFIS had two hidden layers of six nodes each. The input and output layer configurations were the same as in the BPN implementation.

PREDICTIVE MODELING: EMPIRICAL AND PHYSICS-BASED

While our primary interest is in cutting force prediction, we would also like to gain some physical insights into the process of chip formation that are useful in subsequent modeling of cutting temperatures, tool wear, etc. In particular, three types of additional physical insights are possible: (i) insights regarding how the total cutting forces are partitioned and, hence, of the magnitudes of normal and friction forces acting at the chip-tool (rake side) and work-tool (clearance side) interfaces; (ii) insights regarding the shearing process (e.g., knowledge of the work material invariants such as τ and s) provided that ϕ has been empirically determined. Hence, these are also at level 0.

Tables 2 to 6 summarize the equations used in the data analysis (column 2), parameter modeling (column 3), and prediction phases (column 4) of the two empirical and fourteen analytical modeling approaches that we have assessed so far.

Table 2. Implementation details of purely empirical modeling approaches.

Appr.	Data analysis equation sequence	Modeling and Db	Prediction equation sequence
EU	$F_{rf} = f_{Crf} \sin \gamma + f_{Trf} \cos \gamma$	K_{rf}, μ_{rf} : UoIFun (Physics level: 0)	$N_{rf} = K_{rf} t_c w_c$
EP	$N_{rf} = f_{Crf} \cos \gamma - f_{Trf} \sin \gamma$ $K_{rf} = N_{rf} / A_c$ $\mu_{rf} = F_{rf} / N_{rf}$	K_{rf}, μ_{rf} : PowerFun (Physics level: 0)	$F_{rf} = \mu_{rf} N_{rf}$ $f_C = F_{rf} \sin \gamma + N_{rf} \cos \gamma$ $f_T = F_{rf} \cos \gamma - N_{rf} \sin \gamma$

Table 3. Implementation details for approaches inspired by the analytical models of Kobayashi and Thomsen [16-18].

Appr.	Data analysis equation sequence	Modeling and Db	Prediction equation sequence
KT1	$A_c = w_c t_c$ $A_s = A_c / \sin \phi_m$ $F_s = f_C \cos \phi_m - f_T \sin \phi_m$ $f_{rf} = f_C \sin \gamma + f_T \cos \gamma$	Regress F_s against A_s . τ_{Db} = regression line slope. F_{s0Db} = regression line intercept. ELinSAS(ϕ_m) μ_{rf} : UoIFun (Physics level: 2)	$\xi = \tau_{Db} A_c / f_C$ $\beta = \arctan(\mu_{rf})$ $\theta = \beta - \gamma$ $\lambda = \phi + \theta$ $\eta = \{\sin(2\phi + \theta) - \sin \theta\} / (1 - \sin \theta)$ $f_C = \{\tau_{Db} A_c + F_{s0Db} \sin \phi\} / \eta \{2 \cos \theta / (1 - \sin \theta)\}$
KT2	$N_{rf} = f_C \cos \gamma - f_T \sin \gamma$ $\mu_{rf} = F_{rf} / N_{rf}$	Same as for KT1, except that μ_{rf} : PowerFun (Physics level: 2)	

KT3	<p>For each iteration, assume ELinSAS coefficients and find trial ϕ.</p> <p>Now follow procedure for KT1 and KT2 but using ϕ for ϕ_m.</p>	<p>ELinSAS(min scatter(F_s vs A_s regression line). Regress F_s against A_s. τ_{Db}=regression line slope. $F_{s/Db}$=regression line μ_{rf}: UoIFun (Physics level: 3)</p>	$f_T = f_C \tan \theta$
-----	---	--	-------------------------

Table 4. Implementation details for approaches inspired by the analytical model of Armarego [7].

Appr.	Data analysis equation sequence	Modeling and Db	Prediction equation sequence
Ar1	<p><i>OFTP</i>: Perform linear regression of f_C and f_T against t_c. Intercepts are f_{Ccf} and f_{Tcf}.</p> $f_{Crf} = f_C - f_{Ccf}$ $f_{Trf} = N_{cf} = f_T - f_{Tcf}$	$\mu_{r,f}$, \bar{N}_{cf} , and $f_{Tcf} = \bar{N}_{cf} w_c$: UoIFun $\tau_{Db} = \text{mean}(\tau)$ $\phi = \text{ELinSAS}(\phi_m)$ (Physics level: 2)	$A_s = A_c / \sin \phi_m$ $F_s = \tau_{Db} A_s$ $\beta = \arctan \mu_{r,f}$ $\theta = \beta - \gamma$ $R_{rf} = F_s / \tan(\phi + \theta)$ $f_{crf} = R_{rf} \cos \theta$ $f_{Trf} = R_{rf} \sin \theta$
Ar2	$A_c = t_c w_c$ $A_s = A_c / \sin \phi_m$	$\mu_{r,f}$, \bar{N}_{cf} , $\mu_{c,f}$: PowerFun Rest as for Ar1. (Physics level: 2)	$f_{Tcf} = N_{cf} = \bar{N}_{cf} w_c$ $f_{Ccf} = \mu_{r,f} f_{Tcf}$ $f_C = f_{Crf} + f_{Ccf}$ $f_T = f_{Trf} + f_{Tcf}$
Ar3	$F_{rf} = f_{Crf} \sin \gamma + f_{Trf} \cos \gamma$ $N_{rf} = f_{Crf} \cos \gamma - f_{Trf} \sin \gamma$	$\mu_{r,f}$, \bar{N}_{cf} , $\mu_{c,f}$: UoIFun $\tau_{Db} = \text{mean}(\tau)$ $\phi = \text{ELinSAS}(\text{MVMl}(\tau))$ (Physics level: 3)	
Ar4	$F_{cf} = f_{Ccf}$ $\bar{N}_{cf} = N_{cf} / w_c$ $K_{rf} = N_{rf} / A_c$ $\mu_{rf} = F_{rf} / N_{rf}$ $\mu_{cf} = F_{cf} / N_{cf}$ $\beta = \arctan \mu_{r,f}$ $\theta = \beta - \gamma$ $F_s = f_{Crf} \cos \phi_m - f_{Trf} \sin \phi_m$ $\tau = F_s / A_s$	$\mu_{r,f}$, \bar{N}_{cf} , $\mu_{c,f}$: PowerFun Rest as for Ar3. (Physics level: 3)	

Table 5. Implementation details for approaches inspired by the analytical model of Rubenstein [24, 25].

Aprr..	Data analysis equation sequence	Modeling and Db	Prediction equation sequence
R1	Same as in Table 4 except that instead fining τ , find s as $s=f_{Crf}/\{A_c(\cot\phi_m + 1)\}$	$\mu_{r,f}, \bar{N}_{cf}, \mu_{c,f}$: UoIFun $s_{Db}=\text{mean}(s)$ $\phi=\text{ELinSAS}(\phi_m)$ (Physics level: 2)	$f_{Crf} = s_{Db} A_c(\cot\phi+1)$ $\beta=\arctan\mu_{r,f}$ $\theta=\beta-\gamma$ $f_{Trf} = f_{Crf}\tan\theta$ $f_{Tcf} = N_{cf} = \bar{N}_{cf} w_c$
R2		$K_{rf}, \mu_{r,f}, K_{cf}/w_c$: Power Rest as for R1. (Physics level: 2)	$f_{Ccf} = \mu_{r,f} f_{Tcf}$ $f_c = f_{Crf} + f_{Ccf}$ $f_T = f_{Trf} + f_{Tcf}$
R3		$\mu_{r,f}, \bar{N}_{cf}, \mu_{c,f}$: UoIFun $s_{Db}=\text{mean}(s)$ $\phi=\text{ELinSAS}(\text{MVMI}(s))$ (Physics level: 3)	
R4		$\mu_{r,f}, \bar{N}_{cf}, \mu_{c,f}$: PowerFun Rest as for R3. (Physics level: 3)	

Table 6. Implementation details for approaches inspired by the semi-analytical model of Endres, Devor, and Kapoor [14, 15].

Aprr.	Data analysis equation sequence	Modeling and Db	Prediction equation sequence
EDK1	$A_c = t_c w_c$	Optimize UoIFun coefficients of $K_{rf}, \mu_{r,f}$ \bar{N}_{cf} and $\mu_{c,f}$ for minimum rmse of $\{f_c, f_T\}$ prediction. (Physics level: 1)	$N_{rf} = K_{rf} t_c w_c$ $F_{rf} = \mu_{rf} N_{rf}$ $f_{Tcf} = N_{cf} = \bar{N}_{cf} w_c$ $f_{Ccf} = \mu_{cf} f_{Tcf}$ $f_c = f_{Crf} + f_{Ccf}$ $f_T = f_{Trf} + f_{Tcf}$
EDK2		Start for EDK1. Then $\tau_{Db}=\text{mean}(\tau)$ $\phi=\text{ELinSAS}(\text{MVMI}(\tau))$ (Physics level: 3)	Same as for Ar1 in Table 4.
EDK3		Start as for EDK1. Then: $s_{Db}=\text{mean}(s)$. $\phi=\text{ELinSAS}(\text{MVMI}(s))$ (Physics level: 3)	Same as for R1 in Table 5.

Approach EU in Table 2 uses UoIFun as the empirical modeling function whereas approach EP uses PowerFun. Hence, these are also at level 0. The analytical approaches vary in terms of levels of insight (see column 4 of the table).

The analytical approaches vary in terms of levels of physical insight (see column 3 of each table). Approaches KT1 to KT3 (in Table 3) are inspired by the works of Kobayashi and Thomsen, Ar1 to Ar4 (in Table 4) of Armarego, R1 to R4 (in Table 5) of Rubenstein, and EDK1 to EDK3 (in Table 6) of Endres, DeVor, and Kapoor. The reader may obtain an understanding of the basic theories behind the approach summarized in each table by perusing the references cited in the corresponding table title.

With respect to each approach, the following procedure is repeated over all the data records of each dataset. Firstly each data record, k (of dataset j), is processed using the analytical version of each modeling approach as given in column 3 of Tables 2 to 6. This step yields the particular subset of the set of model parameters (e.g., K_{rf} , μ_{rf} , μ_{ef} , τ and/or s) pertinent to the particular modeling approach. Next, these are numerically modeled as UoIFun or PowerFun by applying the corresponding nonlinear regression technique. At the same time, the measured shear angles over the dataset are either modeled using ELinSAS, or a theoretically plausible shear angle distribution of the ELinSAS form estimated through MVMI. The key equations utilized during this phase are listed in column 4. The resulting model coefficients are stored in a database for retrieval during a subsequent force prediction exercise. Column 4 lists the key equations involved in the prediction phase. Essentially, these equations are reorganized versions of the corresponding analytical equations listed in column 2.

ASSESSMENT RESULTS AND DISCUSSION

Table 7 shows the rms force prediction errors (in N) obtained from the 18 modeling approaches with respect to each of the 12 datasets listed in Table 1. For each approach, the aggregate relative force prediction effectiveness values (ARFPE) calculated over all the datasets are shown in the last column. Note that some approaches have failed over certain datasets. Whenever a failure has occurred, the reason for the failure is indicted by a code (F1, F2, etc.) in the corresponding cell in Table 7. The nature of failure corresponding to each code is described briefly in Table 8.

It is seen that dataset 1 (compiled by Eggleston *et al.* [28]) is the only one over which no failures have been observed. Therefore, it is not surprising that several modelers have used this dataset to validate their ideas. Dataset 2 has also fared well. Note that both datasets 1 and 2 are fairly large in size. With the exception of dataset 3, the remaining datasets are of much smaller size. This

reinforces the earlier observation about the desirability of working with as large a dataset as possible.

Table 7. Performance of the 18 approaches over the 12 datasets detailed in Table 1.

Appr.	e_{ij} (N) over dataset j												ARFPE
	1	2	3	4	5	6	7	8	9	10	11	12	
BPN	51	38	15	P_2	19	17	71	40	55	50	42	105	0.81
ANFIS	44	23	14	P_1	P_1	17	71	40	P_1	P_3	160	P_1	0.71
EU	74	60	33	F_1	F_1	21	76	41	F_1	119	369	F_1	0.43
EP	83	F_1	38	47	25	22	76	41	154	132	F_1	265	0.46
KT1	76	52	82	F_1	F_1	NA	NA	NA	F_1	F_2	2399	F_1	0.25
KT2	77	52	94	58	36	NA	NA	NA	254	F_5	2243	415	0.33
KT3	70	47	38	F_1	F_1	13	49	28	F_1	92	324	F_1	0.51
Ar1	102	80	F_4	F_1	F_1	NA	NA	NA	F_1	836	2957	F_1	0.17
Ar2	104	346	F_5	131	26	NA	NA	NA	136	228	1557	305	0.23
Ar3	110	60	62	F_1	F_1	19	76	27	F_1	863	F_5	F_1	0.36
Ar4	138	367	38	130	26	19	73	26	140	158	F_4	287	0.42
R1	115	86	F_5	F_1	F_1	NA	NA	NA	F_1	848	3304	F_1	0.15
R2	108	330	F_5	130	41	NA	NA	NA	127	258	1954	296	0.21
R3	95	60	49	F_1	F_1	17	80	29	F_1	842	5071	F_1	0.38
R4	117	373	30	128	27	14	73	25	135	157	4067	260	0.46
EDK1	63	43	25	48	23	18	72	40	644	73	226	183	0.63
EDK2	72	44	130	49	79	F_2	F_3	F_3	660	1182	233	193	0.34
EDK3	72	43	111	49	75	F_2	F_3	F_3	661	1000	234	187	0.34

NA: Not applicable because measured ϕ values are not available in the dataset.
Note: $\min(e_{ij})$ for each dataset is shown in bold font.

As anticipated in the previous section, the force prediction performances of the two ANN-based approaches are significantly superior to those observed with respect to the 16 empirical/analytical approaches. With its ARFPE equal to 0.81, the performance of BPN is quite impressive. However, there is always the possibility that, on small sized datasets, BPN has ended up memorizing data rather than recognizing patterns implicit in the data. Further work is needed to establish how well this approaches scales up.

Table 8. Descriptions of the failure codes in Table 7.

Code	Reason for failure
F1	Numerical modeling of K_{rf} , μ_{rf} , μ_{cf} or \bar{N}_{cf} could not proceed.
F2	Optimization routine did not converge.
F3	Zero values of ϕ encountered due to programming problems.
F4	'Divide by zero' encountered due to programming problems.
P1	Dataset does not include sufficiently wide range of γ .
P2	Insufficient number of records in the dataset.
P3	Suspected memorization rather than generalization by the ANN.

Although, ANFIS has failed to produce acceptable results on five of the twelve datasets, its ARFPE value of 0.71 is close that of BPN. However, note that when the number of records is large (such as in datasets 1, 2 and 3), ANFIS has performed better than BPN.

ANFIS has yielded rms force prediction error values of 44, 23, and 14N over datasets 1, 2, and 3 respectively (the larger datasets). We may therefore take these values as the upper bounds on the data errors contained in the two datasets (recall our earlier observation that an ANN is not embedded with any physical knowledge about the process being modeled—hence it neither interprets nor misinterprets the process). Dataset 1 has SAE1112 as the work material in 'as received' state whereas dataset 2 uses the same work material but in the annealed state. The work material in dataset can be expected to be more uniform as well as softer. This might be the reason for the lower value of e_{ij} associated with dataset 2.

Sidestepping approaches KT3 and EDK1 for the moment, the two empirical approaches 1 and 2 exhibit the two next best performances. These approaches are purely empirical in nature, hence, devoid of any physical insights. In contrast to approach EDK1, these cannot even partition the cutting forces. Yet they exhibit inferior performances. Could it be that there is a compromise between the level of force prediction effectiveness of a model and the degree of detail to which the model can provide physical insights?

In fact, with ARFPE equal to 0.51, approach KT3 has outperformed the two empirical approaches. The analytical part of this approach generally follows the ideas originally developed by Kobayashi and Thomsen [16-18] in the early 1960s. Thus it is the earliest of the analytical approaches listed in Tables 2 to 6. The approach is rich from the viewpoint of physical insights with regard to

parameters such as ϕ and τ . Yet, it is able to predict forces in a superior manner (it is at level 3).

Although they were developed subsequently, with ARFPE values 0.17 and 0.15 respectively, approaches Ar1 and R1 have fared quite poorly. The poor performances seem to arise from the fact that no optimization procedures have been adopted. Force partitioning is based on the simplistic notion of LFPT prior to parameter modeling. This results in $\mu_{r,f}$, \bar{N}_{cf} , and/or $\mu_{c,f}$ being associated with much scatter so that the subsequent modeling of these parameters using UoIFun is associated with much error. As a result, the predicted friction angle, β , sometimes exhibits too much scatter for an ELinSAS to be fitted in a reliable manner. However, from a procedural viewpoint, Rubenstein's approach is easier to implement because the determination of s needs only f_C and ϕ to be known.

Approaches KT2, Ar2 and R2 differ from KT1, Ar1 and R1 respectively only with regard to the empirical function used for modeling analytically derived parameters K_{rf} , μ_{rf} , \bar{N}_{cf} , and μ_{cf} (PowerFun substitutes UoIFun). Note that in each case, there is an improvement in the ARFPE value. Interestingly, although UoIFun is of more recent origin, its performance is not any better. However, it is possible that there are superior functions waiting to be discovered.

Among the empirical/analytical approaches, approach EDK1 has demonstrated the best performance. This approach adopts a simplified version of the 'dual mechanism' theory proposed more recently by Endres, DeVor and Kapoor [14, 15]. The original approach had used UoIFun to model five force-related analytical parameters for the purpose of arriving at an optimized force partitioning that minimized the force prediction error over a dataset. Our implementation (OFPT) however ignores the possible variation in the cutting edge roundness. As a result, the number of model parameters to be estimated is reduced by one. However, despite the simplifications, the ARFPE value of 0.63 for approach EDK1 is quite large. The approach has been able to model all the twelve datasets (the rms error value of 644N is quite large for dataset 9 because the number of data records is small). Further, over eight of the twelve datasets, its performance is next only to those of the two ANN-based approaches. The main reason for this is that the approach uses an optimized force partitioning technique (OFPT).

Figure 5 indicates that the rms error of EDK1 over dataset 1 is 63N. We have already noted that, over this dataset, ANFIS has achieved the lowest rms error value equal to 44N. This figure must be close to the data error since, as already noted, this dataset exhibits a fairly regular behavior. This suggests that the modeling error associated with EDK1 is of the order of $(63^2 - 44^2)^{0.5} = 45\text{N}$, a value that is of the order of the data error.

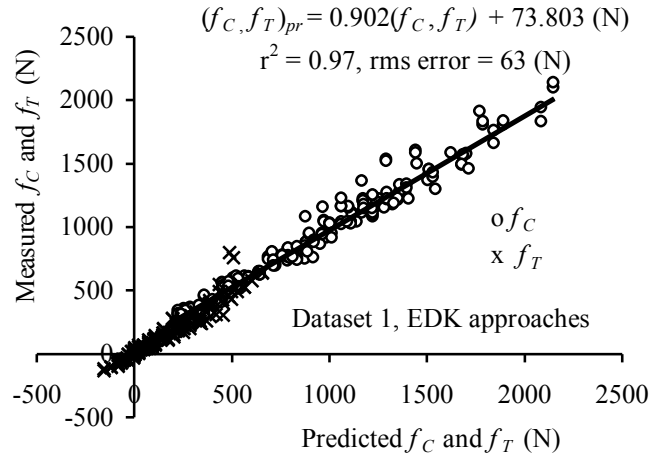


Figure 5. Force prediction accuracies of EDK approaches.

Figure 6 illustrates the variation of the optimally partitioned rake-side cutting force, f_{Crf} , over dataset 1 as estimated from approach EDK1 (and its sequels EDK2 and EDK3). Note that the trends of f_{Crf} are in broad agreement with expectations from traditional cutting theories: increasing with increasing t_c , decreasing with increasing γ , and being relatively insensitive to changes in V . Similar general agreement was also obtained when the f_{Trf} values were plotted. Further, the trends of the apparent chip-tool coefficient of friction, μ_{rf} , have also been found to be in accordance with expectations (see Figure 7): slightly decreasing with increasing t_c , and increasing with increasing γ and V . Further, all μ_{rf} values are in the range 0.4 to 0.8.

Literature on clearance-side forces has been relatively sparse compared to that on rake-side forces. Among the few papers available, the ‘dual mechanism’ paper of Endres, DeVor and Kapoor [14, 15] seems to provide the greatest insights. Although the actual magnitudes are somewhat different, our observations (see Figures 8 and 9) with regard to clearance force variations are in qualitative agreement with those in [15]. Note from Figure 8 that, as expected from general cutting theory, f_{Tcf} is relatively insensitive to t_c . Likewise, it decreases with increasing rake angle. The most interesting observation however is that the tool-work penetration force decreases substantially at higher cutting speeds—probably due to temperature-dependent softening of work surface layers as they approach the rounded cutting edge [14, 15]. Similar trends have been observed with regard to the clearance-side friction force, f_{Ccf} , except that its decrease with increasing cutting speed is less pronounced. This means that the clearance-side coefficient of friction, μ_{cf} , can reach unexpectedly high magnitudes (as high as 30,000!). Further research is needed to fully appreciate the validity and implications of these observations.

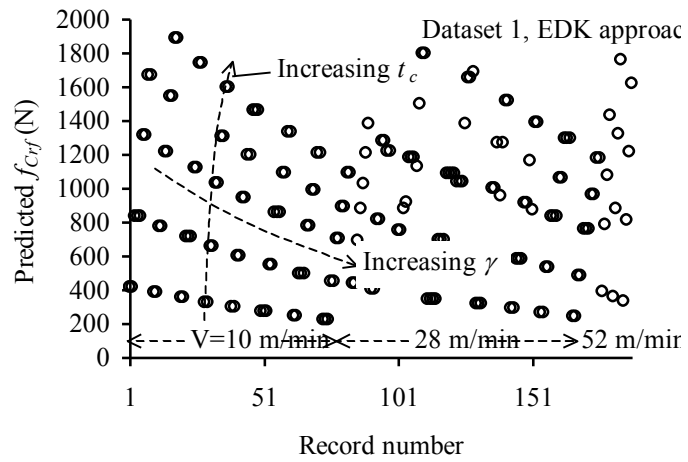


Figure 6. Variation of f_{crf} as predicted from the EDK approaches.

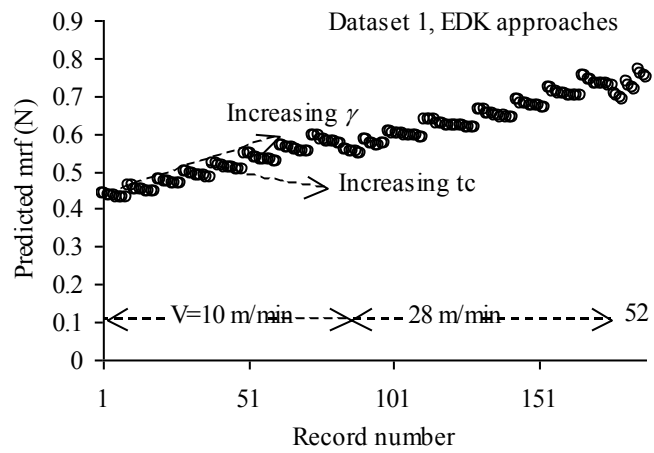


Figure 7. Variation of μ_{rf} as predicted from the EDK approaches.

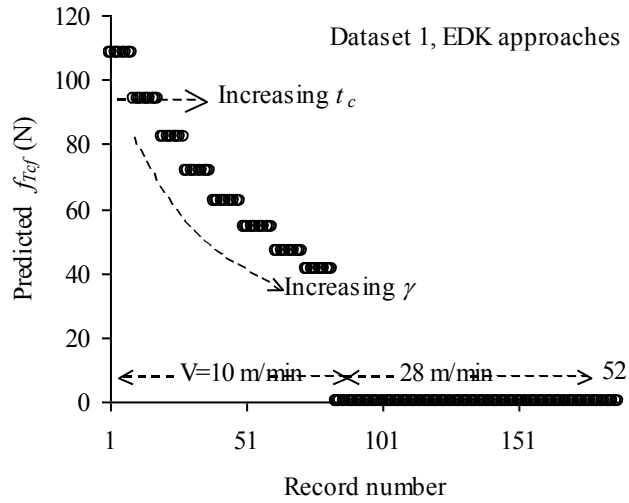


Figure 8. Variation of f_{Tcf} as predicted from the EDK approaches.

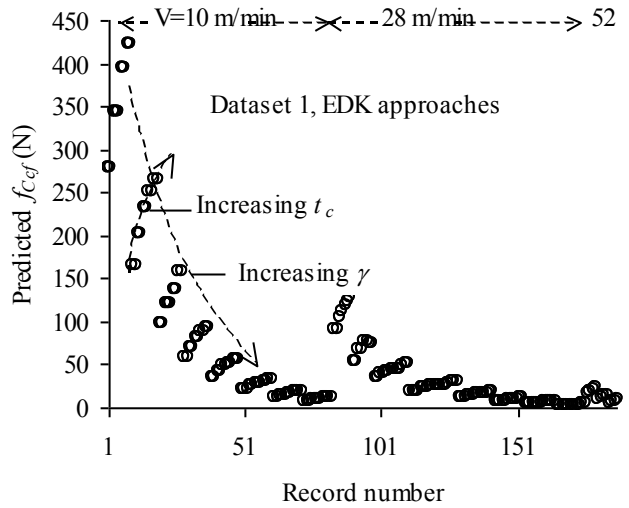


Figure 9. Variation of f_{Ccf} as predicted from the EDK approaches.

Consider now the prediction of shear angle that is of much significance in downstream modeling activities aimed at predicting cutting temperature, tool wear, etc. From this viewpoint, compare the ARFPE values of approaches Ar1 and Ar3. The only difference between the two approaches is that the former is based on measured shear angle values whereas the latter utilizes theoretically estimated values obtained through the minimization of the variation of

Armargeo’s work material invariant, τ (recall MVMI). Note that the ARFPE value for Ar3 (=0.36) is significantly higher than the figure (=0.17) achieved by Ar1. This suggests that ϕ values obtained from MVMI are superior to measured values. This conclusion is reinforced every other time we replace the classical approach with MVMI—compare the ARFPE values yielded by Ar2 with Ar4, by R1 with that by R3, by R2 with that by R4, and by KT1 with that by KT3. This conclusion is of much practical significance since shear angle measurement is a process that is not easily automated.

Returning to our discussion of EDK1, clearly, the approach is useful if the intention is merely to predict cutting forces. On the other hand, owing to its ‘mechanistic’ nature, it can only provide physical insights at level 1—it does not give any information regarding the shearing phenomenon leading to chip formation. However, the approach does yield the optimally partitioned rake and clearance side forces. Hence, we may determine the shear angle from the rake-side forces, f_{Cr} and f_{Tr} , by adopting the previously described ELinSAS/MVMI procedure where MVMI is implemented by minimizing the fractional variation of either (EDK2) τ or s (EDK3). Once, ϕ has been determined thus, it is an easy step to estimate parameters such as τ and s related to the shear plane/zone.

Figure 10 compares the ϕ values predicted by EDK2 and KT3 over dataset 1 with the corresponding measured shear angle values. Note that the performance of EDK2 is significantly superior to that of KT3. The rms error of 3.8 (deg) resulting from EDK2 is much smaller than the 11 deg. yielded by KT3. The former figure is quite plausible when we keep in mind the previously discussed practical errors and theoretical uncertainties associated with the measurement of chip dimensions. Note also from Table 7 that EDK2 has performed better than EDK3.

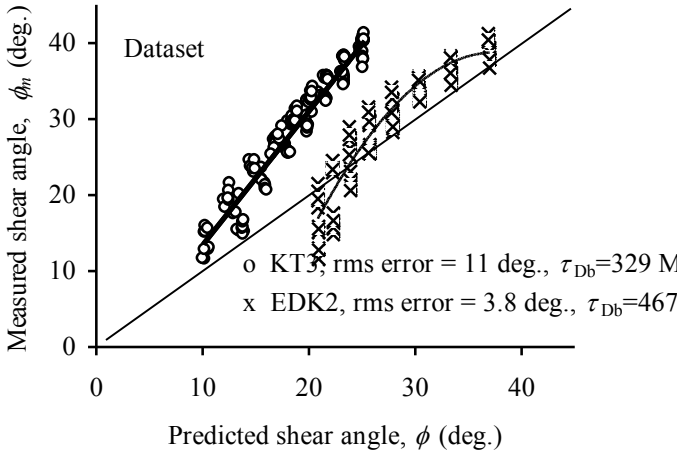


Figure10. Correlation between predicted and measured shear angles.

EDK2 and EDK3 involve optimum force partitioning through OFPT followed by optimum shear angle selection through ELinSAS/MVMI. However, it should be possible (at least in principle) to carry out the two optimization procedures in ‘one shot’ so as to arrive at a more plausible shear angle prediction. However, unfortunately, our attempts to implement such a ‘one shot’ procedure have met with convergence problems owing to the need for determining a much larger number of model coefficients simultaneously. Further research is required to resolve this issue.

CONCLUSIONS

Modeling approaches may be classified into three types. Level 0 models merely facilitate cutting force prediction. Level 1 models enable cutting force partitioning between the rake and, hence, provide insights regarding friction conditions at the chip-tool and work-tool interfaces. Level 2 models provide additional insights regarding parameters related to the shearing process that leads to chip formation provided that empirical shear angle values are known. Level 3 models do the same but without the need for measuring shear angles. In contrast to levels 0 and 1, levels 2 and 3 are capable of facilitating down stream modeling activities directed towards the estimation of cutting temperatures, tool wear, etc. ANN-based and empirical models are level 0 models. Analytical models provide insights at level 1 and above.

The present paper has also compared two numerical functions called UoIFun and PowerFun that can be used to model cutting force related analytical parameters. Regarding shear angle distributions, arguments have been presented in favor of utilizing a new function called the extended linear shear angle solution (ELinSAS).

In the absence of a ‘perfect’ dataset, it is impossible to assess a model’s effectiveness with regard to cutting force prediction in an absolute manner. Hence, a relativistic approach has been developed for estimating the ‘aggregate relative force prediction effectiveness (ARFPE)’ of a given predictive model.

Traditional analytical models have all required chip dimensions to be measured for the purpose of estimating the shear angle. Such measurement is not easily automated and, hence, has become the greatest hurdle to enabling the compilation of autonomous machining databases and cutting force prediction by each individual machine on the shop floor. This problem has been resolved in the present paper by ‘minimizing the variation of the notional work material invariant (MVMI)’ in combination with ELinSAS and subject to Hill’s classical constraints.

In all, two ANN-based (BPN and ANFIS) models, two empirical (UoIFun and PowerFun) models, and fourteen analytical models based on the cutting theories of Armarego, Rubsenstein, DeVor and Kapoor, and Kobayashi and Thomsen have been subjected to comparative assessment.

The two ANN-based approaches have been found to outperform the empirical and analytical models. When the dataset is large, ANFIS can perform better than BPN.

Certain analytical models outperform empirical models although, like ANN-based models, the latter are devoid of any physical insights and, hence, are not limited by any erroneous assumptions regarding the physics of the process.

With regard to modeling of analytically determined process parameters, PowerFun has outperformed UoIFun.

With regard to schools of analytical modeling, that of DeVor and Kapoor has outperformed much better, mainly because it uses an optimized force partitioning technique. However, on its own, this model is unable to predict shear angles.

With regard to analytical models at levels 2 and 3 that depend on measured shear angles, the approach following the ideas of Kobayashi and Thomsen has performed much better than those following the ideas of Armarego and Rubenstein. The main reason for the poor performance of the latter approaches seems to be that force partitioning via the assumption of a linear cutting force *versus* cut thickness relationship leads to undue scatter in model parameters.

The shear angle values estimated via ELinSAS and MVMI leads to much superior cutting force predictions. This superiority is much more evident when the datasets are large. Having arrived at a method for estimating shear angles from cutting force data alone, each machine tool on the shop floor can now be endowed with the ability to predict cutting forces on the basis of data collected from its own normal shop floor experiences.

Several issues identified in the paper require further research. An example is the need for carrying out in ‘one shot’ the optimization procedures directed at force partitioning, and shear angle determination.

ACKNOWLEDGMENT

The authors thank City University of Hong Kong for the facilities and support provided for this study.

REFERENCES

1. *Machining Data Handbook*, 3rd Edition, Vol. 1 and 2, Metcut Research Associates Inc., Cincinnati, Ohio, USA, (1980).
2. R.W. Ivester, M. Kennedy, R. Davies, R. Stevenson, J. Thiele, R. Furness, R., and S. Athavale, “Assessment of Machining Models: Progress Report,” Proc. 3rd CIRP Int.

- Workshop on Modelling of Machining Operations, U. of New South Wales, Sydney, Australia, 20 August, (2000).
3. C.A. van Luttervelt, Opening Statement, Proc. 3rd CIRP Int. Workshop on Modelling of Machining Operations, U. of New South Wales, Sydney, Australia, 20 August, (2000).
 4. C.A. van Luttervelt, T.H.C. Childs, I.S. Jawahir, F. Klocke, and P.K. Venuvinod, "Modeling of Machining Operations," *Annals of the CIRP*, 47(2) (1998) 587-626.
 5. E.J.A. Armarego, "Machining Performance Prediction for Modern Manufacturing," 7th Int. Conf. on High Technology, Chiba, Japan, Advanced Intelligent Production, JSME, (1995) K 52-61.
 6. Z.-Q. Liu, and P.K. Venuvinod, "Error Compensation in CNC Turning Solely from Dimensional Measurements of Previously Machined Parts," *Annals of the CIRP*, 48(1) (1999) 429-432.
 7. E.J.A. Armarego, *Material Removal Processes: An Intermediate Course*, U. of Melbourne, Melbourne, Australia, (1992).
 8. E.J.A. Armarego, and N.P. Deshpande, "Computerized End Milling Force predictions with Cutting Models Allowing For Eccentricity and Cutter Deflections," *Annals of the CIRP*, 40(1) (1991) 25.
 9. E.J.A. Armarego, and H. Zhao, "Predictive Force Models For Point Thinned and Circular Centre Edge Twist Drill Design," *Annals of the CIRP*, 45(1) (1996) 65-70.
 10. M.E. Merchant, "Mechanics of the Metal Cutting Process, I. Orthogonal Cutting and a Type 2 Chip," *J. Appl. Physics*, 16(5) (1945) 267-274.
 11. M.E. Merchant, "Mechanics of the Metal Cutting Process II, Plasticity Conditions in Orthogonal Cutting," *J. Appl. Physics*, 16(6) (1945) 318.
 12. R. Hill, *Mathematical Theory of Plasticity*, Oxford University Press, England, (1950) 134.
 13. R. Hill, "The Mechanics of Machining: A New Approach," *J. Mechanics and Physics of Solids*, 3 (1954) 47-53.
 14. W.J. Endres, R.E. DeVor, and S.G. Kapoor, "A Dual-Mechanism Approach to the Prediction of Machining Forces, Part 1: Model Development," *Trans. ASME*, 117 (1995) 523-533.
 15. W.J. Endres, R.E. DeVor, and S.G. Kapoor, "A Dual-Mechanism Approach to the Prediction of Machining Forces, Part 2: Calibration and Validation," *Trans. ASME*, 117 (1995) 534-541.
 16. S. Kobayashi, and E.G. Thomsen, "Some Observations on the Shearing Process in Metal Cutting," *ASME J. Eng. Ind.*, 81 (1959) 251-262.
 17. S. Kobayashi, S., Thomsen, E.G., "Metal-Cutting Analysis—II Evaluation and New method of Presentation of Theories," *ASME J. Eng. Ind.*, 84 (1962) 63-70.
 18. S. Kobayashi, and E.G. Thomsen, "Metal-Cutting Analysis—II New Parameters," *ASME J. Eng. Ind.*, 84 (1962) 71-80.
 19. J.D. Cumming, S. Kobayashi, S., and E.G. Thomsen, "A New Analysis of the Forces in Orthogonal Metal Cutting," *ASME J. Eng. Ind.*, (1985) 480-486.
 20. P.L.B. Oxley, and M.J.M. Welsh, "Calculating the Shear Angle in Orthogonal Metal Cutting from Fundamental Stress, Strain, Strain-Rate Properties of the Work Material," Proc. 4th Int. Mach. Tool Des. Res. Conf., Pergamon Press, Oxford, (1973).
 21. P.L.B. Oxley, and A.P. Hatton, "Shear Angle Solution Based on Experimental Shear Zone and Tool-Chip Interface Stress Distribution," *Int. J. of Mech. Sci.*, 5 (1963) 41.
 22. P.L.B. Oxley, *The Mechanics of Machining: An Analytical Approach to Assessing Machinability*, Ellis Horwood Ltd., Chichester, Sussex, England, (1989).

23. J.A. Arsecularatne, and P.L.B. Oxley, Prediction of Cutting Forces in Machining with Restricted Contact Tools, *Machining Science and Technology*, 1(1) (1997) 95-112.
24. R. Connolly, and C. Rubenstein, "The Mechanics of Continuous Chip Formation in Orthogonal Cutting," *Int. J. Mach. Tool Des. Res.*, Pergamon Press, 8 (1968) 159-187.
25. C. Rubenstein, "The Application of Force Equilibrium Criteria to Orthogonal Cutting," *Int. J. Mach. Tool Des. Res.*, Pergamon Press, 12 (1972) 121-126.
26. M.K. Cheng, and P.K. Venuvinod, "Development of Autonomous Machining Database at the Machine Level (Part 1)—Cutting Force Data Acquisition through Motor Current Sensing, Int. Conf. Production Res.," (ICPR-16), Prague, Czech Republic, August, (2001).
27. W.J. Endres, *A Dual Mechanism Approach to the Prediction of Machining Forces in Metal-Cutting Processes*, PhD Thesis, University of Illinois at Urbana-Champaign, USA, (1992).
28. D.P. Eggleston, R.P. Herzog, and E.G. Thomsen, "Observations on the Angle Relationships in Metal Cutting," *ASME J. Eng. Ind.*, 81 (1959) 263-279.
29. S. Gottfried, S., and J. Weisman, *Introduction to Optimization Theory*, Prentice-Hall, Inc., Englewood-Cliffs, N.J., USA, (1973).
30. E.H. Lee, and B.W. Schaffer, "The Theory of Plasticity Applied to a Problem of Machining," *J. App. Mech.*, 18(4) (1951) 405.
31. J.T. Lapsley Jr., R.C. Grassi, and E.G. Thomsen, "Correlation of Plastic Deformation During Metal Cutting with Tensile Properties of the Work Material," *Trans. ASME*, 72 (1950) 979-986.
32. D. Kececioglu, "Force Components, Chip Geometry, and Specific Cutting Energy in Orthogonal and Oblique Machining of SAE 1015 Steel," *Trans. ASME*, 80 (1958) 149-157.
33. J.H. Crawford, and M.E. Merchant, "The Influence of Higher Rake Angles on Performance in Milling," *Trans. ASME*, 75 (1953) 561-566.
34. J.S.R. Jang, "Adaptive Network Based Fuzzy Inference Systems," *IEEE Trans. Systems, Man, and Cybernetics*, 23(3) (1993) 665-685.
35. X. Li, P.K. Venuvinod, and M.K. Cheng, "Feed Cutting Force Estimation from the Current Measurement with Hybrid Learning," *Int. J. Adv. Manuf. Tech.*, 16 (2000) 859-862.
36. X. Li, P.K. Venuvinod, Djordjevich, and Z.-Q. Liu, "Predicting Machining Errors in Turning Using Hybrid Learning," *Int. J. Adv. Manuf. Tech.*, 18 (2001) 853-872.